The American Journal of Pathology, Vol. 174, No. 5, May 2009

DOI: 10.2353/ajpath.2009.080055

Metabolic, Endocrine and Genitourinary Pathobiology

PTEN Deficiency Is Fully Penetrant for Prostate Adenocarcinoma in C57BL/6 Mice via mTOR-Dependent Growth

Jorge Blando,* Melisa Portis,* Fernando Benavides,* Angela Alexander,* Gordon Mills,† Bhuvanesh Dave,* Claudio J. Conti,* Jeri Kim,‡ and Cheryl Lyn Walker*

From the Department of Carcinogenesis, Science Park, Research Division, Smithville; and the Departments of Systems Biology,† and Genitourinary Medical Oncology,‡ University of Texas M. D. Anderson Cancer Center, Houston, Texas*

The tumor suppressor phosphatase and tensin homolog (PTEN) is frequently involved in human prostate carcinoma. PTEN is therefore an attractive target for the development of preclinical animal models. Prostate intraepithelial neoplasia lesions develop in mice with *Pten* heterozygosity, but disease progression has been reported only in combination with either other tumor suppressor gene alterations or the conditional inactivation of both *Pten* alleles in prostate epithelial cells. We report that on a C57BL/6 background, in contrast to previous studies on mixed 129 genetic backgrounds, *Pten* locus heterozygosity is fully penetrant for the development of prostate adenocarcinoma. Grossly observable tumors were detected at 6 months of age, and, by 10 to 12 months, 100% of examined mice developed adenocarcinoma of the anterior prostate. Furthermore, double heterozygotes carrying both *Pten* and *Tsc2*-null alleles showed no increase relative to $Pten^{+/-}$ heterozygotes in either lesion development or progression. Lesions in both $Pten^{+/-}$; $Tsc2^{+/-}$, and $Pten^{+/-}$ mice exhibited loss of PTEN expression and activation of PI3K signaling. PI3K activation occurred early in prostate intraepithelial neoplasia lesion formation in these animals, consistent with loss of PTEN function, and contributed to the etiology of tumors that developed in $Pten^{+/-}$ mice. Furthermore, prostate lesion growth in $Pten^{+/-}$ mice was dependent on mTOR, as evidenced by a reduction in both phospho-S6 levels and proliferative index after rapamycin treatment. ***(Am J Pathol 2009, 174:1869–1879; DOI: 10.2353/ajpath.2009.080055)***

The tumor suppressor gene phosphatase and tensin homolog (*PTEN*), also known as *MMAC1* (for mutated in multiple advanced cancers),[1] functions as a lipid and protein phosphatase, inhibiting the ability of PDK1 to activate AKT.[2–4] Loss of PTEN function results in constitutive AKT activation and phosphorylation of downstream targets, including the tuberous sclerosis complex 2 (*TSC2*) tumor suppressor.[5–8] TSC2 inhibits mTOR signaling by functioning as a GTPase activating protein for the small GTPase Rheb, which activates mTOR.[9–11] Phosphorylation of TSC2 by AKT at S939 and S981 causes it to partition into the cytosol away from its target Rheb and its activation partner TSC1 in the membrane, relieving repression of mTOR.[12] Loss of PTEN function therefore results in functional inactivation of the TSC2 protein via AKT phosphorylation, resulting in activation of mTOR signaling.[9]

Loss of one PTEN allele is a high frequency event in prostate cancer, occurring in as many as 70 to 80% of primary tumors[13–16] and homozygous inactivation of PTEN is associated with advanced disease and metastasis.[15,17–19] *Pten* knockout mice (heterozygous $Pten^{+/-}$) develop prostate intraepithelial neoplasia (PIN) with a variable penetrance ranging from 40 to 50%[20–22] to 90%.[23] Lesions develop primarily in the dorsolateral prostate and anterior prostate but appear to spare the ventral prostate. Importantly, progression to adenocarcinoma generally is not observed in $Pten^{+/-}$ mice, possibly due to age-dependent morbidity associated with the high incidence of thyroid lymphomas that occur in these ani-

This study made use of the Research Animal Support Facility - Smithville, Genetic Services, which is supported by P30 CA16672-30 DHHS/NCI Cancer Center Support Grant to M. D. Anderson Cancer Center, the Histology and Tissue Processing Facility Core of the Center for Research on Environmental Disease, supported by grant ES007784, and was supported in part by prostate cancer SPORE P50 CA90270.

Accepted for publication January 27, 2009.

Supplemental material for this article can be found on *http://ajp.amjpathol.org*.

Address reprint requests to Cheryl L. Walker, University of Texas M. D. Anderson Cancer Center, P.O. Box 389, Smithville, Texas 78957. E-mail: chwalker@mdanderson.org.

mals. It has recently been suggested that genetic background and/or modifier genes may influence the development of lesions in *Pten*-haploinsufficient animals.[23] In that study, both onset and spectrum of lesions at several anatomical sites observed with a *Pten* null allele placed on a 129;BALB/c mixed background differed from that observed with *Pten* null alleles on either a 129;C57BL/6 or 129;CD-1 mixed backgrounds.

In contrast to *Pten* heterozygotes, conditional *Pten* knockout mice with complete loss of Pten in the prostate develop invasive prostate carcinoma, with variable latency.[24–28] Inactivation of *Pten* in combination with other mutations can also promote cancer progression. Double heterozygous mice that carry *p27* (now *Cdkn1b*) and *Pten* defects ($Pten^{+/-}$, $p27^{+/-}$) develop invasive carcinoma.[29] Similarly, when crossed with *Nkx3–1* knockout mice (a homeobox gene expressed in prostate epithelium) $Nkx3\text{–}1^{+/-}$, $Pten^{+/-}$ mice also develop metastatic prostate carcinoma.[30,31] Heterozygosity at the *Pten* locus also promotes prostate cancer progression in the transgenic murine prostate cancer model (TRAMP)[32] and conditional *Pten* knockouts crossed with *p53* (*Trp53*) knockouts develop highly lethal invasive prostate carcinoma at a young age.[33] Recently, other alterations that regulate PTEN/PI3K signaling at the level of mTOR have also been shown to contribute to prostate carcinogenesis: Pten haploinsufficiency cooperates with Rheb overexpression to promote prostate tumorigenesis[34] and Lkb1 deficiency, a tumor suppressor and upstream kinase for AMP-activated kinase signaling to TSC2, leads to the development of PIN lesions.[35]

TSC2 has not been previously implicated in prostate tumorigenesis, but alterations in this tumor suppressor gene do predispose to genitourinary tumors, primarily renal cell carcinoma.[36] *Tsc2* knockout mice develop renal cell carcinoma and vascular lesions, primarily liver hemangiomas, but do not develop prostate lesions, even at older ages.[37,38] Interestingly, it was recently reported that $Pten^{+/-}$;$Tsc2^{+/-}$ double heterozygous mice develop invasive prostate carcinoma with 100% penetrance.[39] In this study, tumors were reported to arise as early as 5 months of age and were found in all lobes of the prostate (dorsolateral prostate, anterior prostate, and ventral prostate). *Pten* expression from the normal allele was reported to be retained in these tumors, suggesting that the *Tsc2* defect was responsible for progression of *Pten*-dependent prostate cancer in these animals. However, a similar study using $Pten^{+/-}$;$Tsc2^{+/-}$ mice reported no progression of PIN lesions in double heterozygotes.[40] Thus the potential for *Tsc2* defects to contribute to the development of *Pten*-dependent prostate carcinoma requires further study.

We report here that in contrast to previous studies in which *Pten* null alleles were placed on mixed 129 genetic backgrounds, *Pten* haploinsufficiency is fully penetrant for development of prostate carcinoma on a C57BL/6 background. 100% of $Pten^{+/-}$ mice developed prostate adenocarcinoma by 10–12 months of age. Furthermore, double heterozygotes carrying both *Pten* and *Tsc2* null alleles did not exhibit any acceleration in lesion development or progression. Activated mTOR signaling that could be reversed with rapamycin was observed in PIN lesions and adenocarcinomas that developed in $Pten^{+/-}$ animals, with adenocarcinomas from both $Pten^{+/-}$;$Tsc2^{+/-}$ and $Pten^{+/-}$ mice exhibiting loss of PTEN expression.

Materials and Methods

In Vivo *Studies*

Mice were housed in suspended polycarbonate cages or individually ventilated cages (Lab Products, Maywood, NJ) on autoclaved hardwood bedding (PJ Murphy Forest Products Corp., Montville, NJ) in an AAALAC-accredited facility (M. D. Anderson Cancer Center, Science Park–Research Division). Room conditions included temperature (20–22°C), humidity (60–70%), and light (14/10 hours; light/dark). Commercial rodent pelleted food (Harlan Teklad, Madison, WI) and autoclaved water were available *ad libitum*. All procedures were in compliance with the Public Health Service Guide for the Care and Use of Laboratory Animals (National Research Council, 1996). The protocol involving use of these mice was approved by the M. D. Anderson Cancer Center Institutional Animal Care and Use Committee. Male mice were euthanized at various ages from 7 to 12 months by CO_2 asphyxiation, and tissues were harvested and either snap-frozen in liquid N_2 and stored at −80°C or fixed in 10% neutral buffered formalin and paraffin embedded. The intact male reproductive system was transversely sectioned and then paraffin-embedded for histopathological and immunohistological analysis. The $Pten^{+/-}$ mice were a kind gift from Dr. Ramone Parsons (Columbia University)[20] and the $Tsc2^{+/-}$ mice were obtained from Dr. David Kwiatkowski (Brigham and Women's Hospital).[38]

$Pten^{+/-}$ *Mice Treated with Vehicle and Rapamycin*

$Pten^{+/-}$ mice 12 to 14 months old were treated with rapamycin (LC Laboratories, Woburn, MA) (0.15 mg/kg) ($n = 4$) or vehicle ($n = 3$) for 14 days daily (i.p) and sacrificed at the end of the study. The vehicle was Tween 80, polyethylene glycol, and ethanol). Tissues were harvested and fixed as described above.

Genetic Background Characterization of C57BL/6-Pten Mice

We performed a genetic background characterization of our C57BL/6.129S1/v-*Pten* congenic strain containing a *Pten* targeted mutation ($Pten^{tm1Rps}$).[20] For this, we selected 92 microsatellite markers (simple sequence length polymorphism) evenly distributed over all of the 19 autosomal chromosomes (genome scan) and polymorphic between C57BL/6J and 129S1/Sv inbred strains. The average marker spacing was 15 cM. D19Mit88 on chromosome 19 was the only marker showing 129S1/C57BL/6 heterozygosity for all $Pten^{+/-}$ mice. This is expected

since the *Pten* gene is localized in the same region on chromosome 19 as D19Mit88, and the targeted allele is 129S1/Sv (W9.5 ES cells) in origin. In agreement with the number of backcross generations performed in our *Pten* null colony (>N6), the background strain characterization showed that 91 of 92 markers (98.9%) were homozygous C57BL/6.

Histological Analysis

Tissues were stained with hematoxylin and eosin, and prostates were examined microscopically by two study pathologists (J.B. and C.J.C.) blinded as to age and genotype of study animals. Hematoxylin and eosin sections were evaluated for precursor lesions identified as hyperplastic, low-grade PIN, or high-grade PIN and adenocarcinoma whose severity was described by Shapell et al.[41] To detect downstream targets of the PTEN signaling pathway, immunohistochemistry was performed on paraffin-embedded prostate tissue sections using primary antibodies against AKT (1:100; Santa Cruz no. sc-1619, Santa Cruz, CA), phospho-AKT (Ser 473) (1:50; Cell Signaling Technologies, Beverly, MA, no. 3787), S6 (1:50; Cell Signaling Technologies no. 2217), and phospho-S6 (S235/236) (1:50; Cell Signaling Technologies no. 2211). Ki-67 (1:50 Santa Cruz no.15402) was used to determine proliferative index in vehicle and rapamycin treated mice. Primary antibodies were detected with biotinylated secondary antibodies, including anti-goat IgG for AKT, and an Envision plus labeled polymer, anti-rabbit-horseradish peroxidase (Dako Laboratories, Carpinteria, CA), for phospho-AKT, S6 and phospho-S6. This was followed by peroxidase-conjugated avidin/biotin (Vectastain ABC Kit, Vector Laboratories, Burlingame, CA) and DAB substrate (Dako Laboratories). Intensity of immunohistochemistry staining was graded on a scale as follows: "-" indicating no apparent staining, "+" indicating weak staining, "++" indicating moderate staining and "+++" indicating strong staining. The four point scale for grading immunohistochemistry was used as described previously.[42,43]

For detection of PTEN, after deparaffinization, sections were pretreated with microwave irradiation in 0.01 mol/L citrate buffer (pH 6.0), followed by blocking 20 minutes with 10% normal donkey serum. Sections were incubated with anti-PTEN antibody (Neomarkers, 1:50 dilution, Freemont, CA) overnight at 4°C. After washing with phosphate-buffered saline, the sections were incubated with the secondary fluorescein isothiocyanate-conjugated donkey anti-mouse IgG (1:200; Jackson ImmunoResearch Laboratories, West Grove, PA). The slides were examined using a Fluoroview laser confocal microscope (Olympus America, Melville, NY).

Western Analysis

Normal and tumorigenic anterior prostate tissue lysates were subjected to sodium dodecyl sulfate-polyacrylamide gel electrophoresis and transferred to polyvinylidene difluoride membranes. Membranes were blocked with 5% nonfat dry milk and separately incubated with phospho-AKT (Thr 308) (1:1000, Cell Signaling Technologies), phospho-AKT (Ser 473) AKT (1:1000, Cell Signaling Technologies), (1:1000, Cell Signaling Technologies), phospho-S6 (1:2000, Cell Signaling Technologies), S6 (1:1000, Cell Signaling Technologies), phospho-TSC2 (Ser 939) (1:1000, Cell Signaling Technologies), and TSC2 (1:1000, Epitomics; Burlingame, CA) for 2 hours, followed by streptavidin horseradish peroxidase-conjugated goat anti-rabbit secondary antibody for one hour at room temperature. Lumiglo (KPL) was used for detection on X-ray film (BioMax, Eastman Kodak, Rochester, NY). As a loading control, blots were stripped and reprobed with an antibody to γ-tubulin (1:5000; Sigma, St. Louis, MO).

Results

C57BL/6-Pten$^{+/-}$ Mice Develop Prostate Adenocarcinoma

In-house colonies of *Pten*$^{+/-}$[20] and *Tsc2*$^{+/-}$[38] mice maintained on a C57BL/6 genetic background and confirmed by microsatellite analysis to be homozygous C57BL/6 (see Materials and Methods) were used to generate double heterozygous mice (*Pten*$^{+/-}$; *Tsc2*$^{+/-}$) for analysis. Prostate lesions were evaluated in wild-type, *Pten*$^{+/-}$ single heterozygotes, *Pten*$^{+/-}$; *Tsc2*$^{+/-}$ double heterozygotes and *Tsc2*$^{+/-}$ single heterozygotes with groups of male mice examined at 7–9 and 10–12 months of age.

Table 1. Adenocarcinoma Incidence in the Prostate

	wt			*Pten*$^{+/-}$			*Pten Tsc2*			*Tsc2*$^{+/-}$		
	n	No. of lesions		*n*	No. of lesions		*n*	No. of lesions		*n*	No. of lesion	
7–9 months												
AP	4	0	0%	11	7	64%	9	3	33%	10	0	0.0%
VP	5	0	0%	10	2	20%	9	3	33%	10	0	0.0%
DLP	2	0	0%	10	3	30%	9	3	33%	10	0	0.0%
SV	5	0	0%	11	0	0%	9	0	0	10	0	0.0%
10–12 months												
AP	5	0	0%	8	8	100%	9	8	89%	14	0	0.0%
VP	6	0	0%	6	2	33%	9	2	20%	14	0	0.0%
DLP	6	0	0%	6	4	67%	9	3	33%	14	0	0.0%
SV	6	0	0%	7	1	14%	9	3	33%	14	0	0.0%

In two age groups, 7–9 months and 10–12 months, the number of lesions was counted in four regions of the male reproductive system. AP, anterior prostate; VP, ventral prostate; DLP, dorsolateral prostate; SV, seminal vesicle. *n* = number of prostates examined that contained the region of interest.

Whole prostates were removed from mice and processed using conventional histology techniques. At necropsy, grossly observable prostate lesions were often noted, in one case in a moribund animal at 6 months of age. As shown in Supplemental Figure 1 (found at *http://ajp.amjpathol.org*), enlargement and changes in the coloration and texture of the anterior prostrate were the most common observations in these animals. Large, solid masses were also observed, often adjacent to the bladder, which were later confirmed to be tumors arising from the ventral prostate. Although at a lower frequency, grossly observable lesions were also identified in the dorsolateral prostate and seminal vesicle.

Histological analysis confirmed the neoplastic nature of grossly observable lesions and allowed the identification of a variety of microscopic lesions in all three lobes of the prostate. The adenocarcinomas observed in both the 7–9 and 10–12 month groups were moderately to well differentiated, forming in some cases large neoplastic masses with ill-defined glandular structures. Tumors with neuroendocrine differentiation or poorly differentiated histology were not observed.

As shown in Table 1 and Figure 1, adenocarcinomas were observed in the anterior prostates of 100% of the *Pten*$^{+/-}$ male mice by 12 months of age, whereas no wild-type or *Tsc2*$^{+/-}$ mice developed these lesions. While complete penetrance for adenocarcinoma was observed in the anterior prostate of *Pten*$^{+/-}$ mice, adenocarcinomas also arose in the ventral and dorsolateral prostates of 33% and 67% of heterozygous mice, respectively, and in seminal vesicles of 14% of *Pten*$^{+/-}$ and 33% of *Pten*$^{+/-}$;*Tsc2*$^{+/-}$ mice (Figure 1, A–F). Seminal vesicles with invasive adenocarcinoma and intraepithelial neoplasia exhibited similar features and cytological characteristics as lesions arising in other lobes of the prostate (Figure 1, G–J). Double heterozygous *Pten*$^{+/-}$;*Tsc2*$^{+/-}$ animals failed to exhibit any increased incidence of adenocarcinoma relative to *Pten*$^{+/-}$ mice. Thus, in the anterior prostate the *Pten* null allele was fully penetrant for development of prostate adenocarcinoma, and the presence of a *Tsc2* null allele did not accelerate lesion development throughout the prostate.

Prostate Cancer Progression in C57BL/6-Pten$^{+/-}$ *Mice*

Precursor lesions for prostate adenocarcinoma were also evaluated microscopically. As shown in Table 2 the anterior prostates of wild-type, *Pten*$^{+/-}$ and *Pten*$^{+/-}$;*Tsc2*$^{+/-}$, and *Tsc2*$^{+/-}$ mice presented with hyperplasia, characterized by increased number of acini and increased epithelial tufting (Figure 1). In addition, a significant number of animals carrying the Pten-null allele showed atypical glandular structures with epithelial stratification and a cribriform pattern, essentially identical to the PIN lesions described previously in Pten$^{+/-}$ mice and other murine models of prostate cancer. These lesions were then further classified as low grade or high-grade PIN (Figure 1, D–F) according to the severity as described by Shapell et al (Bar Harbor Consensus Report).[41]

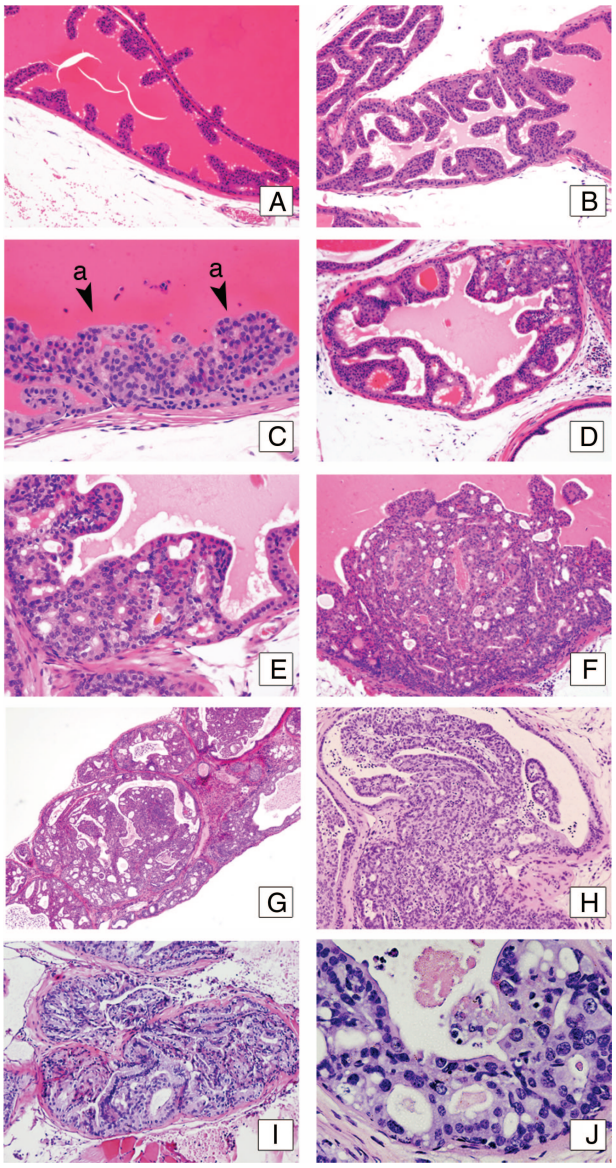

Figure 1. Histology of lesions of the anterior prostate. Sections of 6- to 12-month-old mice. **A:** Anterior prostate from wild-type mouse showing a single stratum of luminal epithelial cells with normal recurrent mucosal folds projecting into the gland. **B** and **C:** Anterior prostate from an 8-month-old *Pten;Tsc2* double heterozygous mouse showing luminal epithelial hyperplasia (**C, a**; **arrowheads**) without cellular atypia. **D** and **E**: Anterior prostate from 12-month-old *Pten* heterozygous mouse. Low-grade PIN lesions presenting stratification of the luminal epithelia with cribriform pattern and moderate cellular atypia. **F:** High-grade PIN from a 12-month-old *Pten;Tsc2* double heterozygous mouse. This lesion displays a highly dysplastic luminal epithelium and the presence of nuclear atypia. **G–I:** Invasive adenocarcinoma from the anterior prostate of a 12-month-old *Pten* heterozygous mouse. Widespread local invasion of moderate to well differentiated tumor cells. **J:** Higher magnification of PIN lesion in the anterior prostate. Note the difference in the sizes of the nucleolus among cells, chromatin condensation, nuclear atypia, and formation of small intraluminal glands. H& E; magnifications: **A**, **B**, **D**, **F**, **G**, ×10; **C**, **E**, **H**, **I**, ×20; **J**, ×40.

As shown in Table 2, hyperplasias were noted in wild-type and in *Tsc2*$^{+/-}$ mice, but progression to PIN lesions was not observed in these animals. *Pten*$^{+/-}$ mice also developed hyperplasia by 7–9 months, but in contrast to wild-type and *Tsc2*$^{+/-}$ animals, these lesions progressed from hyperplasia to more advanced lesions, which also occurred in *Pten*$^{+/-}$; *Tsc2*$^{+/-}$ mice. As shown in Figure

Table 2. Summary of Precursor Lesions in the Prostate

		7–9 months				10–12 months			
		AP	VP	DLP	SV	AP	VP	DLP	SV
WT	Hyperplasia	1/4 (25%)	2/5 (40%)	0/2	0/5	2/5 (40%)	0/6	0/6	0/6
	LGPIN	0/4	0/5	0/2	0/5	0/5	0/6	0/6	0/6
	HGPIN	0/4	0/5	0/2	0/5	0/5	0/6	0/6	0/6
$Pten^{+/-}$	Hyperplasia	3/11 (27%)	3/10 (30%)	2/10 (20%)	1/11 (9%)	0/8	1/6 (17%)	0/6	1/7 (14%)
	LGPIN	6/11 (55%)	1/10 (10%)	4/10 (40%)	0/11	3/8 (38%)	1/6 (17%)	2/6 (33%)	3/7
	HGPIN	1/11 (9%)	4/10 (40%)	0/10	0/11	1/8 (13%)	0/6	1/6 (17%)	0/7
Pten/Tsc2	Hyperplasia	1/9 (11%)	0/9	1/9 (11%)	0/9	0/9	3/10 (30%)	0/9	0/9
	LGPIN	5/9 (55%)	0/9	1/9 (11%)	0/9	5/9 (56%)	0/10	0/9	1/9 (11%)
	HGPIN	1/9 (11%)	0/9	1/9 (11%)	0/9	1/8 (13%)	0/10	1/9 (11%)	3/9 (33%)
$Tsc2^{+/-}$	Hyperplasia	2/10 (20%)	1/10 (10%)	0/10	0/10	1/14 (7%)	2/14 (14%)	2/14 (14%)	0/14
	LGPIN	0/10	0/10	0/10	0/10	0/14	0/14	0/14	0/14
	HGPIN	0/10	0/10	0/10	0/10	0/14	0/11	0/14	0/14

Prostates from animals in two age groups, 7–9 months and 10–12 months, were examined for hyperplasia (HP), low-grade PIN (LGPIN), and high-grade PIN (HGPIN). AP, anterior prostate; VP, ventral prostate; DLP, dorsolateral prostate; SV, seminal vesicle.

2A–F, in both $Pten^{+/-}$ and $Pten^{+/-}$; $Tsc2^{+/-}$ mice, other than differing in their anatomical location, the histology of hyperplasias and PIN lesions observed in the dorsolateral prostate, ventral prostate and intraepithelial neoplasia in seminal vesicles were similar to the cognate lesions observed in the anterior prostate.

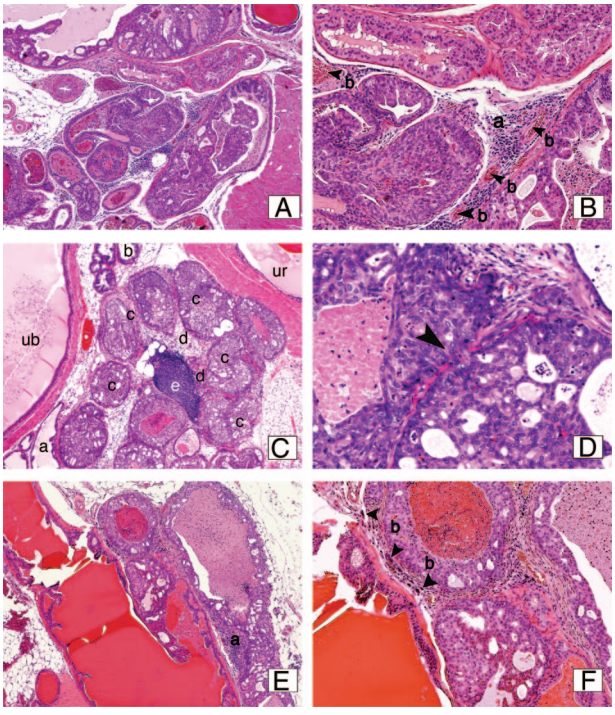

Figure 2. Histology of prostate lesions. **A** and **B:** High-grade PIN and intraepithelial adenocarcinoma derived from the dorsal prostate in an 8-month-old *Pten;Tsc2* double heterozygous mouse. Note the presence of an inflammatory infiltrate (**B**, **a**) as well as increased vascularization (**B**, **b arrowheads**). **C** and **D:** Ventral prostate from a 12-month-old *Pten* heterozygous mouse showing normal glands (**C**, **a**) glands with atypical hyperplasia (**C**, **b**), and a mixed high-grade PIN/adenocarcinoma areas (**C**, **c**) with stromal invasion (**C**, **d**). A lymphocytic infiltration is also present (**C**, **e**) ub, urinary bladder; ur, urethra. **D** shows a higher magnification (×20) of adenocarcinoma with a notable membrane rupture and stromal invasion (**arrowhead**). **E** and **F:** Seminal vesicle from a 12-month-old *Pten* heterozygous mouse with low- and high- grade intraepithelial neoplasia and focal areas of invasive adenocarcinoma (**E**, **a**). The presence of an inflammatory infiltrate is indicated (**F**, **b arrowheads**). H&E; magnifications: ×4 (**A**, **C**, **E**), ×4; **B**, **D**, **F**, ×10.

Loss of Pten Function in Prostate Adenocarcinomas

The PTEN tumor suppressor protein functions to inhibit PI3K/AKT activation. On loss of PTEN function, AKT becomes activated, phosphorylating and inactivating TSC2 to activate other signaling pathways such the mTOR pathway and its effectors, including ribosomal S6. Thus, activation of AKT is a reliable indicator of loss of PTEN function in the prostate.[26] Anterior prostates obtained from animals histologically confirmed to have adenocarcinoma were used to determine AKT activation and mTOR signaling by Western analysis. As shown in Figure 3 and Supplemental Table 1 (found at *http://ajp.amjpathol.org*), all prostates from $Pten^{+/-}$ and $Pten^{+/-}$; $Tsc2^{+/-}$ mice exhibited elevated Akt activity, as as-

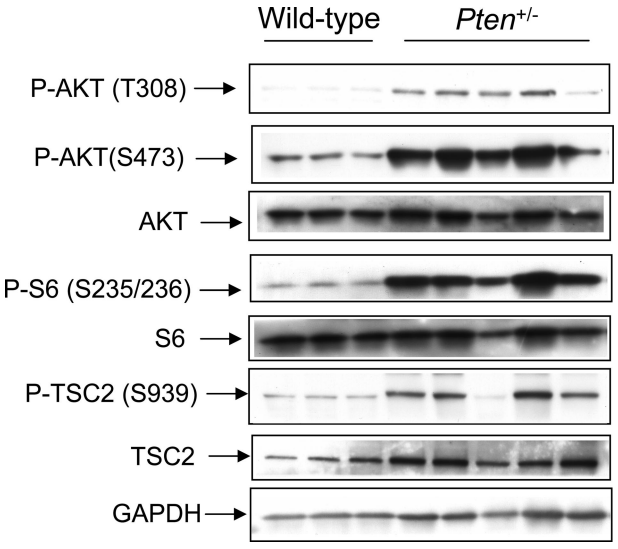

Figure 3. Prostates from tumor-bearing mice exhibit constitutive activation of PI3K/Akt signaling and functional inactivation of Tsc2. Tissue lysates of normal anterior prostate from wild-type mice and prostates of mice with histologically confirmed tumors from *Pten* and *Pten;Tsc2* double heterozygous mice were examined by Western analysis with antibodies for phosphorylated Akt (S473 and T308), S6 (S235/236), Tsc2 (S939), and the corresponding total proteins. After stripping, membranes were probed with GTPase activating proteinDH antibody as a loading control.

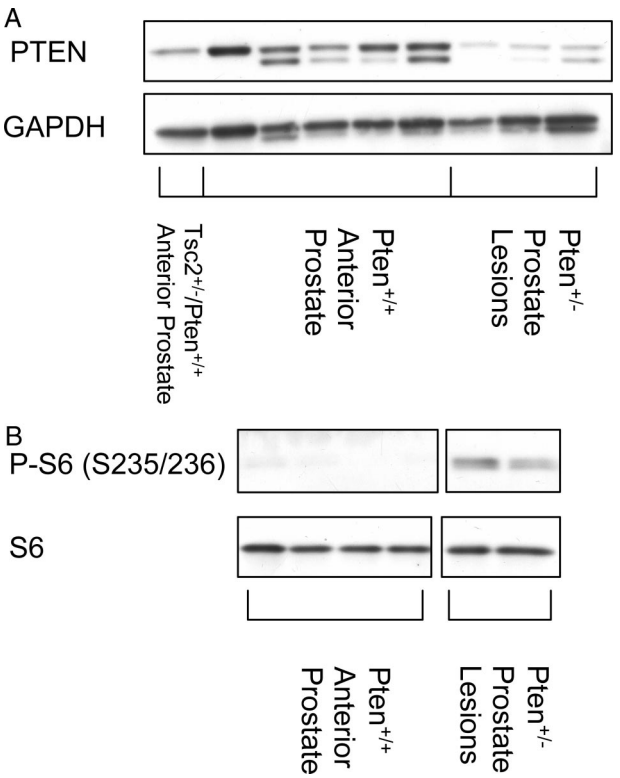

Figure 4. Loss of Pten expression of adenocarcinomas of Pten$^{+/-}$ mice. Anterior prostates and macroscopic tumors were dissected from *Pten*$^{+/-}$, *Pten*$^{+/+}$, and *Pten*$^{+/+}$;*Tsc2*$^{+/-}$ mice. Tissues were examined by Western analysis for expression of Pten (**A**) and phosphorylation of S6 (S235/236) (**B**).

sessed by phosphorylation of Akt at S473 and T308, and/or phosphorylation of S6 and Tsc2. In approximately 50% of the anterior prostate lesions examined, Pten expression was absent or barely detectable (summarized in Supplemental Table 1 at *http://ajp.amjpathol.org*). Importantly, Tsc2 expression was retained in both *Pten*$^{+/-}$ and *Pten*$^{+/-}$; *Tsc2*$^{+/-}$ double heterozygotes, and consistent with loss of PTEN and activation of AKT, was phosphorylated at S939 (Figure 3), indicating functional inactivation of Tsc2 occurred in these lesions rather than loss of heterozygosity.

Because prostates contain both tumor and normal tissues, to determine whether the wild-type *Pten* allele was lost in prostate adenocarcinomas, we isolated macroscopic tumors from *Pten*$^{+/-}$ mice and Western analysis was performed to assess *Pten* expression in these lesions. In addition, we performed immunohistochemistry on anterior prostates from *Pten*$^{+/-}$ mice confirmed to have microscopic adenocarcinomas. Pten expression was lost or barely detectable in adenocarcinomas from *Pten*$^{+/-}$ mice (Figure 4a and Figure 5), consistent with elevated S6 phosphorylation observed in these tumors (Figure 4b) and activation of AKT signaling observed in the prostates of *Pten*$^{+/-}$ animals (Figure 6). Similarly, while normal epithelial cells in the anterior prostate exhibited strong immunoreactivity with an antibody directed against Pten, this was not observed in adenocarcinomas of *Pten*$^{+/-}$ mice (Figure 5).

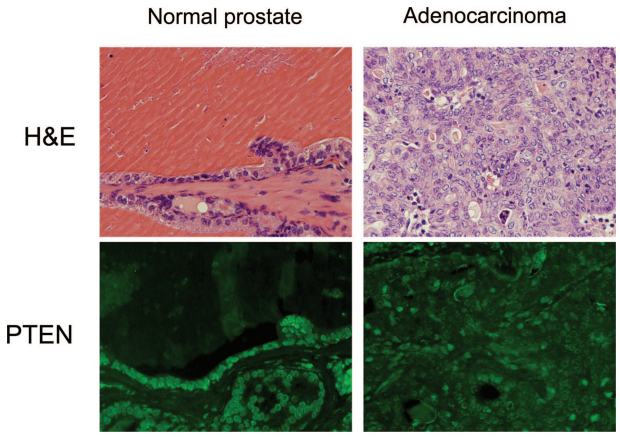

Figure 5. H&E and immunofluorescence detection of PTEN. Adenocarcinoma (**right column**) exhibits little immunoreactivity for PTEN in the nucleus of the neoplastic cells compared with cells in normal glands (**left column**), which have with intense immunoreactivity. Upper panels, H&E; lower panels, immunofluorescence demonstrates immunoreactivity for PTEN.

Progression of Prostate Lesions in Pten-Haploinsufficient Mice Correlates with Elevated AKT and mTOR Signaling

To explore when during the progression of prostate lesions loss of PTEN function and activation of AKT and mTOR signaling occurred, normal prostate and hyperplasias, PIN lesions and adenocarcinomas from *Pten*$^{+/-}$ and *Pten*$^{+/-}$; *Tsc2*$^{+/-}$ mice were stained for phospho-AKT and phospho-S6, markers for loss of PTEN function and mTOR activation, respectively. As shown in Figures 6 and 7, all adenocarcinomas stained positively for phospho-AKT (Ser 473) and phospho-S6 (Ser 235/236), whereas normal anterior prostate was negative for both phospho-AKT and phospho-S6 immunoreactivity. Hyperplasias were also negative for phospho-AKT and phospho-S6, indicating that development of these lesions was not associated with loss of PTEN function, which was also consistent with the presence of hyperplasias as background lesions in this strain. However, PIN lesions that developed in both *Pten*$^{+/-}$ and *Pten*$^{+/-}$; *Tsc2*$^{+/-}$ mice contained detectable levels of phospho-AKT and phospho-S6, indicating that loss of PTEN function had occurred during this stage of progression. Interestingly in concordance with a previous study,[40] in *Pten*$^{+/-}$; Tsc2$^{+/-}$ mice, both high-grade PIN and adenocarcinoma had levels of phospho-AKT that were lower than comparable lesions arising in *Pten*$^{+/-}$ mice. Thus heterozygosity at the *Tsc2* locus appeared to have a dampening effect on AKT activation following loss of PTEN function.

Growth of Prostate Lesions Is mTOR-Dependent

To further understand the implications of elevated mTOR signaling in prostate lesions that develop as a result of loss of PTEN function, we treated *Pten*$^{+/-}$ mice for 14 days with 0.15 mg/kg of rapamycin and stained the prostate for phospho-S6 to monitor mTOR signaling (Figure

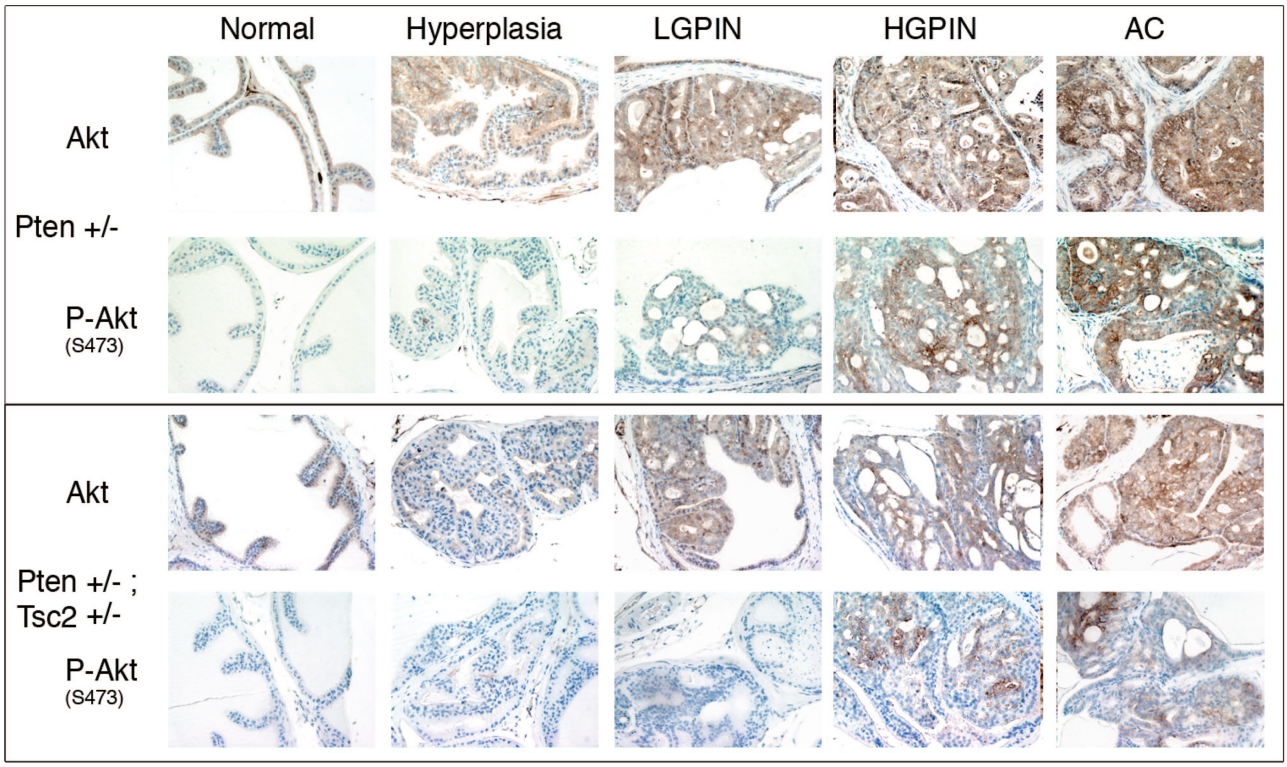

Strain	IHC	Normal	Hyperplasia	LGPIN	HGPIN	AC
Pten +/-	Akt	+	++	++	++	+++
	P-Akt	-	-	+	++	+++
Pten+/-, Tsc2 +/-	Akt	+	+	+	+	++
	P-Akt	-	-	-	+	+

Figure 6. Activation of Akt during prostate tumorigenesis. Sections from *Pten* and *Pten;Tsc2* double heterozygous mice bearing lesions at different stages during tumor development were stained with antibodies to total Akt and phosphorylated Akt (S473). Sections were quantified by the following criteria: −, no staining; +, weak staining; ++, moderate staining; +++, strong staining.

8A). We observed that rapamycin given for even a short duration (14 days) was sufficient to down-regulate mTOR signaling as evidenced by reduction of S6 phosphorylation in PIN lesions and adenocarcinomas. Also, the total number of lesions was reduced in rapamycin-treated mice (Figure 8), although the number of animals examined were too small to evaluate statistically. However, we further investigated the functional significance of inhibition of mTOR signaling by examining cell proliferation (Ki-67 levels) in these lesions (Figure 8, B and C). Dramatic reductions in cell proliferation in response to rapamycin confirmed that these lesions were dependent on mTOR for growth.

Discussion

Loss of the tumor suppressor PTEN is observed in a high percentage of human prostate cancers, making it an important target for the development of preclinical mouse models of this human disease. We found that *Pten* deficiency ($Pten^{+/-}$) was fully penetrant for prostate adenocarcinoma in C57BL/6 mice, in contrast to the previous studies on mixed 129 backgrounds, indicating that the genetic background is important for susceptibility to tumorigenesis. Furthermore, the presence of the *Tsc2*-null allele in double heterozygous $Pten^{+/-}$; $Tsc2^{+/-}$ mice did not alter lesion development or progression. The prostate lesions that progressed beyond hyperplasia had activated PI3K signaling in both $Pten^{+/-}$ single and $Pten^{+/-}$;$Tsc2^{+/-}$ double heterozygotes, as evidenced by downstream activation of AKT and mTOR, indicating that loss of PTEN function was associated with disease progression. Prostate lesions that developed in the *Pten*-deficient mice were dependent on mTOR signaling for growth as demonstrated by inhibition of phospho-S6 levels and reduction in proliferative index in mice treated with rapamycin.

mTOR-dependent growth of lesions in $Pten^{+/-}$ mice is consistent with loss of PTEN function driving tumor progression in this model. In this regard, the phenotype of lesions that develop in $Pten^{+/-}$ mice on a pure C57BL/6 background compares favorably to models where *Pten* is conditionally inactivated in prostate epithelial cells on 129 mixed backgrounds (129/C57BL/6,[24] 129;C57BL/6;DBA; BALB/c,[25,26] and 129;FVB[27]). Similar to what we ob-

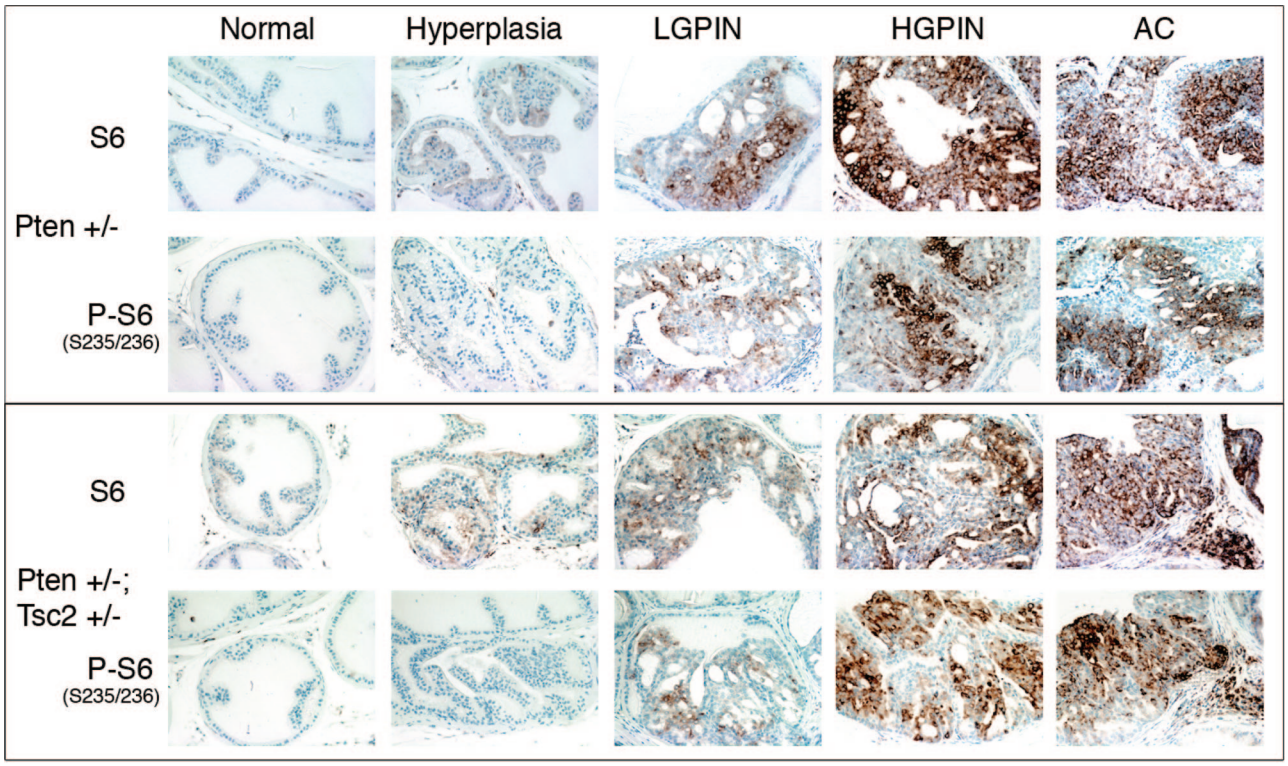

Strain	IHC	Normal	Hyperplasia	LGPIN	HGPIN	AC
Pten +/-	S6	-	+	++	+++	++
	P-S6	-	-	+	++	++
Pten+/-; Tsc2 +/-	S6	-	+	++	+++	++
	P-S6	-	-	+	++	++

Figure 7. Activation of mTOR during prostate tumorigenesis. Sections from *Pten* and *Pten;Tsc2* double heterozygous mice bearing lesions at different stages during tumor development were stained with antibodies to total S6 and phospho-S6 (S235/236). Sections were quantified by the following criteria: −, no staining; +, weak staining; ++, moderate staining; +++, strong staining.

served, in these models bi-allelic loss of *Pten* was fully penetrant for neoplasia (high-grade PIN, prostate carcinoma *in situ*, and invasive prostatic carcinoma), with focal invasion observed with variable latency from 2 to 7 months. The longer latency observed in our study with $Pten^{+/-}$ C57BL/6 mice (complete penetrance by 10–12 months) is consistent with the need for acquisition of a "second hit" at the wild-type *Pten* allele in $Pten^{+/-}$ heterozygotes. In the present report, the underlying mechanism responsible for loss of Pten function (loss of heterozygosity, mutation, etc) was not examined. However, loss of heterozygosity at the Pten locus has been demonstrated to occur in prostate lesions that develop in $Pten^{+/-}$ mice combined with other genetic defects such as overexpression of Fgf8[44] or loss of NKx3.1.[30]

Previous studies in human prostate cancer cells and xenografts in immunocompromised mice demonstrated that the rapamycin analog CCI-779 was effective at suppressing mTOR signaling as evidenced by decreased phospho-S6 levels determined by immunostaining and Western analysis.[45] Further, a reduction in proliferation was observed in xenografts of mice bearing PTEN-negative PC3 cells on treatment with CCI-779, linking mTOR activation on loss of PTEN function to cell growth.[46] Together with our data, these studies demonstrate that *Pten*-deficient preclinical models have utility for evaluating mTOR as a therapeutic target for prostate cancer. Moreover, constitutive activation of AKT in mouse prostatic epithelial cells causes intraepithelial neoplasia, which is reduced on treatment with the mTOR inhibitor RAD001.[47] While cell growth in prostate lesions in $Pten^{+/-}$ mice was dependent on mTOR, the role of other growth factors, or steroid hormones in the development of lesions in $Pten^{+/-}$ mice on the C57BL/6 background remains to be determined. As reviewed by Roy-Burman et al,[48] other signaling pathways including those activated by androgens, fibroblast growth factors and retinoids likely contribute to the growth of tumors in this model.

In mouse models, it is well documented that phenotype can be affected by genetic background. For example, tumor type and onset is very different in BALB/c versus C57BL/6 *Trp53* knockout mice.[49] Recently, background strain has been reported to modify the latency and spectrum of tumors that develop in $Pten^{+/-}$ mice.[23] Further, genetic background may also influence prostate gene expression in mice.[50] In the report from

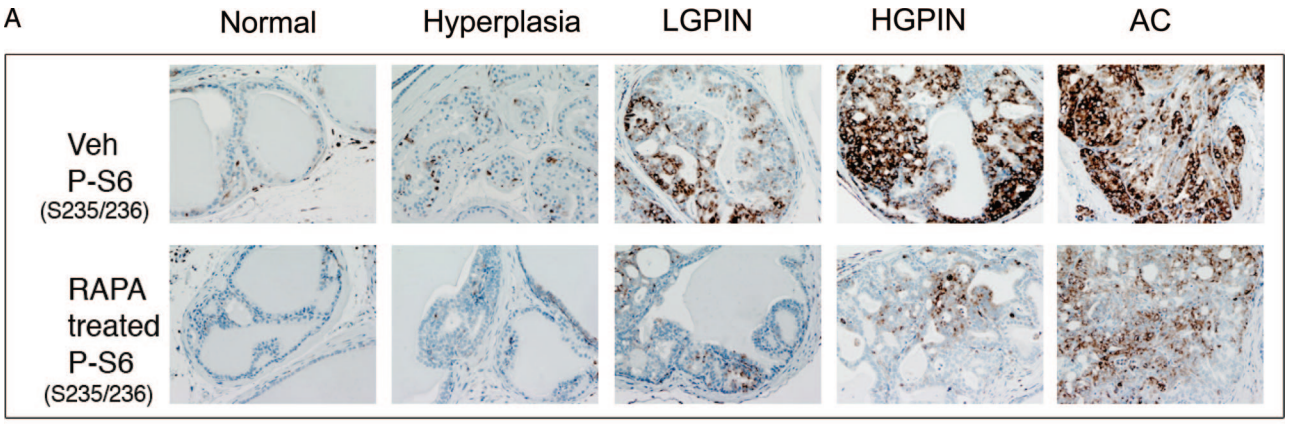

Treatment	IHC	Normal	Hyperplasia	LGPIN	HGPIN	AC
Vehicle	P-S6	+	+	++	+++	+++
Rapamycin	P-S6	-	-	+	+	+

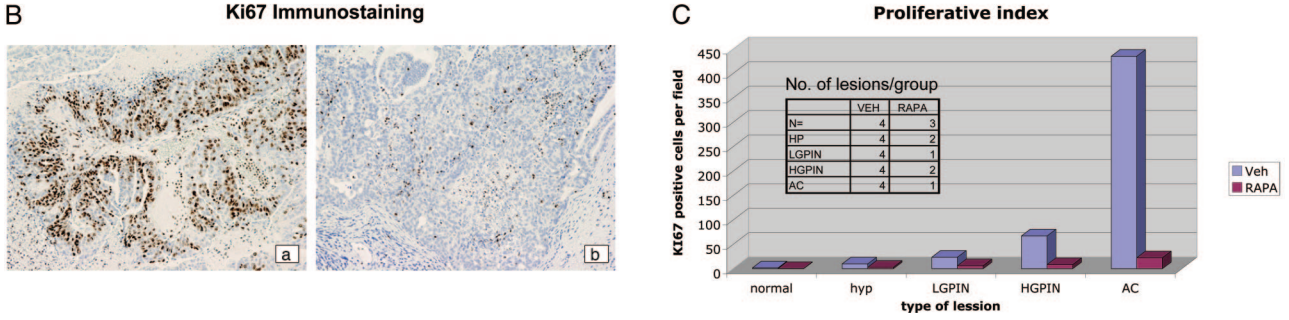

Figure 8. Rapamycin treatment of prostate lesions. Prostate sections from *Pten* $^{+/-}$ mice were stained with antibodies to phosphorylated S6 (P-S6: S235/236) (**A**) and Ki-67 (**B**). Representative staining pattern in mice treated with vehicle versus rapamycin (RAPA) for phospho-S6 (S235/236) (**A**) and Ki-67 (**B**) in vehicle (**a**) versus rapamycin (**b**) treated mice. Phospho-S6 positivity (**A**) was quantified by the following criteria: −, no staining; +, weak staining; ++, moderate staining; +++, strong staining. Sections stained with Ki-67 (**C**) were quantified as number of positive cells per field (magnification, ×10; n = 2–5 fields examined).

Freeman et al,[23] a higher incidence of prostate abnormalities was observed on 129;BALB/c compared with 129;C57BL/6 and 129;CD-1 mixed backgrounds, although the onset of tumor development was delayed. In another prostate cancer model, Kim and collaborators showed that the prostatic phenotype of *Nkx3–1* mutant mice was similar in three congenic lines involving 129S1/Sv, FVB/N, and C57BL/6 backgrounds; however, the incidence of PIN-like lesions was higher in FVB/N and C57BL/6 mice.[51] In this regard, it is interesting to note that, working with a mouse model with prostate-specific expression of human *AKT1*, Xu and colleagues have showed that C57BL/6-*Pbsn-Akt1* transgenic mice have approximately fivefold higher rates of proliferation on the ventral prostate when compared with FVB/N-*Pbsn-Akt1*.[52]

Of interest is our observation that *Pten* $^{+/-}$;*Tsc2* $^{+/-}$ double heterozygous mice do not exhibit any increase in lesion progression relative to *Pten* $^{+/-}$ mice, which differs from the recent report that *Pten* $^{+/-}$;*Tsc2* $^{+/-}$ double heterozygous mice have a higher incidence of prostatic adenocarcinoma than *Pten* $^{+/-}$ mice.[39] However, our study is consistent with the work of others[40] where *Pten* $^{+/-}$; *Tsc2* $^{+/-}$ double heterozygous mice exhibited no increase in prostate lesions relative to *Pten* $^{+/-}$ mice. Likely, part of the difference between these studies is due to the difference in the genetic background of the animals used in our study (C57BL/6J) compared with that of the Pandolfi group (129 mixed background).[39]

Importantly, while existing mouse models in which a germline *Pten* defect is combined with other defined genetic alterations in genes such as *p53*, *Rb*, *p27*, *Nkx3–1*, *Rarg*, and *Stat5a* are valuable for studying disease pathogenesis and prostate cancer progression, they have the inherent property of directing tumor development down specific molecular pathways reflective of subsets of the human disease. In this regard, the availability of *Pten* $^{+/-}$ mice in which the pathways to tumor progression following loss of PTEN function are not constrained may be advantageous as a preclinical model for evaluating therapeutic and preventative strategies for human prostate cancer. Future studies in C57BL/6 *Pten* $^{+/-}$ mice to characterize the spectrum of additional molecular alterations that contribute to disease progression will prove valuable, as will studies aimed at identifying modifier genes present in C57BL/6 and other strains of mice that can modulate prostate cancer progression.

References

1. Steck PA, Pershouse MA, Jasser SA, Yung WK, Lin H, Ligon AH, Langford LA, Baumgard ML, Hattier T, Davis T, Frye C, Hu R, Swedlund B, Teng DH, Tavtigian SV: Identification of a candidate tumour suppressor gene. MMAC1, at chromosome 10q233 that is mutated in multiple advanced cancers. Nat Genet 1997, 15:356–362
2. Cully M, You H, Levine AJ, Mak TW: Beyond PTEN mutations: the PI3K pathway as an integrator of multiple inputs during tumorigenesis. Nat Rev Cancer 2006, 6:184–192
3. Sulis ML, Parsons R: PTEN: from pathology to biology. Trends Cell Biol 2003, 13:478–483
4. Eng C: PTEN: one gene, many syndromes. Hum Mutat 2003, 22: 183–198
5. Altomare DA, Testa JR: Perturbations of the AKT signaling pathway in human cancer. Oncogene 2005, 24:7455–7464
6. Hay N: The Akt-mTOR tango and its relevance to cancer. Cancer Cell 2005, 8:179–183
7. Shaw RJ, Cantley LC: Ras. PI(3)K and mTOR signalling controls tumour cell growth. Nature 2006, 441:424–430
8. Vivanco I, Sawyers CL: The phosphatidylinositol 3-Kinase AKT pathway in human cancer. Nat Rev Cancer 2002, 2:489–501
9. Inoki K, Corradetti MN, Guan KL: Dysregulation of the TSC-mTOR pathway in human disease. Nat Genet 2005, 37:19–24
10. Manning BD, Cantley LC: Rheb fills a GAP between TSC and TOR. Trends Biochem Sci 2003, 28:573–576
11. Li Y, Corradetti MN, Inoki K, Guan KL: TSC2: filling the GAP in the mTOR signaling pathway. Trends Biochem Sci 2004, 29:32–38
12. Cai SL, Tee AR, Short JD, Bergeron JM, Kim J, Shen J, Guo R, Johnson CL, Kiguchi K, Walker CL: Activity of TSC2 is inhibited by AKT-mediated phosphorylation and membrane partitioning. J Cell Biol 2006, 173:279–289
13. Whang YE, Wu X, Suzuki H, Reiter RE, Tran C, Vessella RL, Said JW, Isaacs WB, Sawyers CL: Inactivation of the tumor suppressor PTEN/MMAC1 in advanced human prostate cancer through loss of expression. Proc Natl Acad Sci USA 1998, 95:5246–5250
14. Gray IC, Phillips SM, Lee SJ, Neoptolemos JP, Weissenbach J, Spurr NK: Loss of the chromosomal region 10q23–25 in prostate cancer. Cancer Res 1995, 55:4800–4803
15. Cairns P, Okami K, Halachmi S, Halachmi N, Esteller M, Herman JG, Jen J, Isaacs WB, Bova GS, Sidransky D: Frequent inactivation of PTEN/MMAC1 in primary prostate cancer. Cancer Res 1997, 57:4997–5000
16. Suzuki H, Freije D, Nusskern DR, Okami K, Cairns P, Sidransky D, Isaacs WB, Bova GS: Interfocal heterogeneity of PTEN/MMAC1 gene alterations in multiple metastatic prostate cancer tissues. Cancer Res 1998, 58:204–209
17. Cantley LC, Neel BG: New insights into tumor suppression: PTEN suppresses tumor formation by restraining the phosphoinositide 3-kinase/AKT pathway. Proc Natl Acad Sci USA 1999, 96:4240–4245
18. Di Cristofano A, Pandolfi PP: The multiple roles of PTEN in tumor suppression. Cell 2000, 100:387–390
19. Abate-Shen C, Shen MM: Molecular genetics of prostate cancer. Genes Dev 2000, 14:2410–2434
20. Podsypanina K, Ellenson LH, Nemes A, Gu J, Tamura M, Yamada KM, Cordon-Cardo C, Catoretti G, Fisher PE, Parsons R: Mutation of Pten/Mmac1 in mice causes neoplasia in multiple organ systems. Proc Natl Acad Sci USA 1999, 96:1563–1568
21. Di Cristofano A, Pesce B, Cordon-Cardo C, Pandolfi PP: Pten is essential for embryonic development and tumour suppression. Nat Genet 1998, 19:348–355
22. Stambolic V, Tsao MS, Macpherson D, Suzuki A, Chapman WB, Mak TW: High incidence of breast and endometrial neoplasia resembling human Cowden syndrome in pten+/− mice. Cancer Res 2000, 60:3605–3611
23. Freeman D, Lesche R, Kertesz N, Wang S, Li G, Gao J, Groszer M, Martinez-Diaz H, Rozengurt N, Thomas G, Liu X, Wu H: Genetic background controls tumor development in PTEN-deficient mice. Cancer Res 2006, 66:6492–6496
24. Backman SA, Ghazarian D, So K, Sanchez O, Wagner KU, Hennighausen L, Suzuki A, Tsao MS, Chapman WB, Stambolic V, Mak TW: Early onset of neoplasia in the prostate and skin of mice with tissue-specific deletion of Pten. Proc Natl Acad Sci USA 2004, 101:1725–1730
25. Trotman LC, Niki M, Dotan ZA, Koutcher JA, Di Cristofano A, Xiao A, Khoo AS, Roy-Burman P, Greenberg NM, Van Dyke T, Cordon-Cardo C, Pandolfi PP: Pten dose dictates cancer progression in the prostate. PLoS Biol 2003, 1:E59
26. Wang S, Gao J, Lei Q, Rozengurt N, Pritchard C, Jiao J, Thomas GV, Li G, Roy-Burman P, Nelson PS, Liu X, Wu H: Prostate-specific deletion of the murine Pten tumor suppressor gene leads to metastatic prostate cancer. Cancer Cell 2003, 4:209–221
27. Ma X, Ziel-van der Made AC, Autar B, van der Korput HA, Vermeij M, van Duijn P, Cleutjens KB, de Krijger R, Krimpenfort P, Berns A, van der Kwast TH, Trapman J: Targeted biallelic inactivation of Pten in the mouse prostate leads to prostate cancer accompanied by increased epithelial cell proliferation but not by reduced apoptosis. Cancer Res 2005, 65:5730–5739
28. Ratnacaram CK, Teletin M, Jiang M, Meng X, Chambon P, Metzger D: Temporally controlled ablation of PTEN in adult mouse prostate epithelium generates a model of invasive prostatic adenocarcinoma. Proc Natl Acad Sci USA 2008, 105:2521–2526
29. Di Cristofano A, De Acetis M, Koff A, Cordon-Cardo C, Pandolfi PP: Pten and p27KIP1 cooperate in prostate cancer tumor suppression in the mouse. Nat Genet 2001, 27:222–224
30. Kim MJ, Cardiff RD, Desai N, Banach-Petrosky WA, Parsons R, Shen MM, Abate-Shen C: Cooperativity of Nkx3.1 and Pten loss of function in a mouse model of prostate carcinogenesis. Proc Natl Acad Sci USA 2002, 99:2884–2889
31. Abate-Shen C, Banach-Petrosky WA, Sun X, Economides KD, Desai N, Gregg JP, Borowsky AD, Cardiff RD, Shen MM: Nkx3.1;Pten mutant mice develop invasive prostate adenocarcinoma and lymph node metastases. Cancer Res 2003, 63:3886–3890
32. Kwabi-Addo B, Giri D, Schmidt K, Podsypanina K, Parsons R, Greenberg N, Ittmann M: Haploinsufficiency of the Pten tumor suppressor gene promotes prostate cancer progression. Proc Natl Acad Sci USA 2001, 98:11563–11568
33. Chen Z, Trotman LC, Shaffer D, Lin HK, Dotan ZA, Niki M, Koutcher JA, Scher HI, Ludwig T, Gerald W, Cordon-Cardo C, Pandolfi PP: Crucial role of p53-dependent cellular senescence in suppression of Pten-deficient tumorigenesis. Nature 2005, 436:725–730
34. Nardella C, Chen Z, Salmena L, Carracedo A, Alimonti A, Egia A, Carver B, Gerald W, Cordon-Cardo C, Pandolfi PP: Aberrant Rheb-mediated mTORC1 activation and Pten haploinsufficiency are cooperative oncogenic events. Genes Dev 2008, 22:2172–2177
35. Pearson HB, McCarthy A, Collins CM, Ashworth A, Clarke AR: Lkb1 deficiency causes prostate neoplasia in the mouse. Cancer Res 2008, 68:2223–2232
36. Gomez MR, Sampson JR, Whittemore VH: Tuberous Sclerosis Complex. Edited by Harris JC. Oxford, Oxford University Press, 1999, pp 3–46
37. Kobayashi T, Minowa O, Kuno J, Mitani H, Hino O, Noda T: Renal carcinogenesis, hepatic hemangiomatosis, and embryonic lethality caused by a germ-line Tsc2 mutation in mice. Cancer Res 1999, 59:1206–1211
38. Onda H, Lueck A, Marks PW, Warren HB, Kwiatkowski DJ: Tsc2(+/−) mice develop tumors in multiple sites that express gelsolin and are influenced by genetic background. J Clin Invest 1999, 104:687–695
39. Ma L, Teruya-Feldstein J, Behrendt N, Chen Z, Noda T, Hino O, Cordon-Cardo C, Pandolfi PP: Genetic analysis of Pten and Tsc2 functional interactions in the mouse reveals asymmetrical haploinsufficiency in tumor suppression. Genes Dev 2005, 19:1779–1786
40. Manning BD, Logsdon MN, Lipovsky AI, Abbott D, Kwiatkowski DJ, Cantley LC: Feedback inhibition of Akt signaling limits the growth of tumors lacking Tsc2. Genes Dev 2005, 19:1773–1778
41. Shappell SB, Thomas GV, Roberts RL, Herbert R, Ittmann MM, Rubin MA, Humphrey PA, Sundberg JP, Rozengurt N, Barrios R, Ward JM, Cardiff RD: Prostate pathology of genetically engineered mice: definitions and classification. The consensus report from the Bar Harbor meeting of the Mouse Models of Human Cancer Consortium Prostate Pathology Committee. Cancer Res 2004, 64:2270–2305
42. Maxwell P, McCluggage WG: Audit and internal quality control in immunohistochemistry. J Clin Pathol 2000, 53:929–932
43. Adams EJ, Green JA, Clark AH, Youngson JH: Comparison of different scoring systems for immunohistochemical staining. J Clin Pathol 1999, 52:75–77
44. Zhong C, Saribekyan G, Liao CP, Cohen MB, Roy-Burman P: Coop-

eration between FGF8b overexpression and PTEN deficiency in prostate tumorigenesis. Cancer Res 2006, 66:2188–2194
45. Wu L, Birle DC, Tannock IF: Effects of the mammalian target of rapamycin inhibitor CCI-779 used alone or with chemotherapy on human prostate cancer cells and xenografts. Cancer Res 2005, 65:2825–2831
46. Grunwald V, DeGraffenried L, Russel D, Friedrichs WE, Ray RB, Hidalgo M: Inhibitors of mTOR reverse doxorubicin resistance conferred by PTEN status in prostate cancer cells. Cancer Res 2002, 62:6141–6145
47. Majumder PK, Febbo PG, Bikoff R, Berger R, Xue Q, McMahon LM, Manola J, Brugarolas J, McDonnell TJ, Golub TR, Loda M, Lane HA, Sellers WR: mTOR inhibition reverses Akt-dependent prostate intraepithelial neoplasia through regulation of apoptotic and HIF-1-dependent pathways. Nat Med 2004, 10:594–601
48. Roy-Burman P, Wu H, Powell WC, Hagenkord J, Cohen MB: Genetically defined mouse models that mimic natural aspects of human prostate cancer development. Endocr Relat Cancer 2004, 11: 225–254
49. Kuperwasser C, Hurlbut GD, Kittrell FS, Dickinson ES, Laucirica R, Medina D, Naber SP, Jerry DJ: Development of spontaneous mammary tumors in BALB/c p53 heterozygous mice. A model for Li-Fraumeni syndrome, Am J Pathol 2000, 157:2151–2159
50. Bianchi-Frias D, Pritchard C, Mecham BH, Coleman IM, Nelson PS: Genetic background influences murine prostate gene expression: implications for cancer phenotypes. Genome Biol 2007, 8:R117
51. Kim MJ, Bhatia-Gaur R, Banach-Petrosky WA, Desai N, Wang Y, Hayward SW, Cunha GR, Cardiff RD, Shen MM, Abate-Shen C: Nkx3.1 mutant mice recapitulate early stages of prostate carcinogenesis. Cancer Res 2002, 62:2999–3004
52. Xu Q, Majumder PK, Ross K, Shim Y, Golub TR, Loda M, Sellers WR: Identification of prostate cancer modifier pathways using parental strain expression mapping. Proc Natl Acad Sci USA 2007, 104: 17771–17776